Structural Engineering and Mechanics, *Vol. 52, No. 3 (2014) 469-483*
DOI: http://dx.doi.org/10.12989/sem.2014.52.3.469

Performance analysis of spherical indentation process during loading and unloading - a contact mechanics approach

V. C. Sathish Gandhi[*1], R. Kumaravelan[2a] and S. Ramesh[3b]

[1]*Department of Mechanical Engineering, University College of Engineering Ariyalur, (A constituent College of Anna University, Chennai), Ariyalur - 621 704, Tamilnadu, India*
[2]*Department of Mechanical Engineering, Velalar College of Engineering and Technology, Erode - 638 012, Tamilnadu, India*
[3]*Department of Mechanical Engineering, Vel Tech High Tech Dr. Rangarajan Dr. Sakunthala Engineering College, Chennai - 600 062, Tamilnadu, India*

(Received January 17, 2014, Revised April 15, 2014, Accepted April 28, 2014)

Abstract. In an indentation approach, the smooth rigid spherical ball penetrated into a deformable flat is considered for the study based on contact mechanics approach. The elastic-plastic frictionless spherical indentation analysis has been under taken in the finite element analysis using 'ABAQUS' and experimental study. The spherical indentation has been studied for the materials like steel, aluminium, copper and brass with an identical spherical indenter for diverse indentation depths. The springback analysis is executed for studying the actual indentation depth after the indenter is unloaded. In the springback simulation, the material recovers its elastic deformation after the indenter is unloaded. The residual diameter and depth of an indentation for various materials are measured and compared with simulation results. It shows a good agreement between the simulation and an experimental studies.

Keywords: indentation; elastic-plastic; depth of indentation; springback analysis; indentation diameter; contact mechanics

1. Introduction

Contact mechanics is the study of the deformation of solids that touch each other at one or more points. The theory developed by Hertz (1881) remains the foundation for most contact problems encountered in engineering. It applies to normal contact between two elastic solids that are smooth and can be described locally with orthogonal radii of curvature such as a toroid. The contact of a sphere on a flat surface is a fundamental problem in contact mechanics giving important scientific and technological information. The two different aspects are flattening and indentation approaches. These fundamental approaches have been studied for modelling a single asperity contact either considering a deformable hemisphere in contact with a rigid flat surface (Flattening approach) or by solving the contact mechanics problem of a rigid spherical indenter

∗Corresponding author, Assistant Professor, E-mail: vcsgandhi@gmail.com
[a]Professor, E-mail: rkumaravelan@gmail.com
[b]Professor, E-mail: ramesh_1968in@yahoo.com

http://www.techno-press.org/?journal=sem&subpage=8 ISSN: 1225-4568 (Print), 1598-6217 (Online)

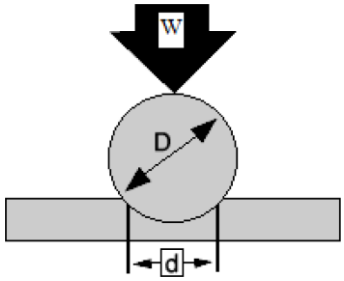

Fig. 1 Rigid sphere model (RS model)

penetrating into a deformable half - space (Indentation approach).

Fig. 1 shows that the RS-model (indentation approach). In the Brinell hardness test a hard ball of diameter 'D' is penetrated under a load 'W' into the plane surface under test. After removal of the load, the chordal diameter 'd' of the resulting indentation is measured. In a sphere and flat contact model, sphere is to be considered as rigid and flat as deformable clearly some applications are better represented by indentation approach. The problem of the contact between a rigid sphere and a deformable flat is considered.

2. Literature review

The studies on indentation approach contact model is carried out based on the type of indenter used for this approach. The studies also carried out based on simulation techniques. The studies mainly focused on the spherical indentation model. Bisrat and Roberts (2000) used Hertzian indentation to measure surface stresses on ceramics. Surface stress in brittle materials have the effect of shifting the minimum load to produce Hertzian fracture. Ahn and Kwon (2001) studied the true stress - true strain relationships of steels with different work-hardening exponents. Cao and Lu (2004) proposed a new methodology to extract the plastic properties of metallic materials from an instrumented spherical indentation loading curve using dimensional analysis and finite element computation. Demir and Sonmez (2004) studied to predict the Brinell hardness distribution in cold formed parts by relating the plastic strains found by finite element analysis to hardness. Lee *et al.* (2005) investigated some inaccuracies and limitations of prior indentation theories, which are based on experimental observation and the deformation theory of plasticity. Habbab *et al.* (2006) presented a finite element simulations of spherical indentations accounting for frictional contact provide validated load-indentation output for assessing and improved existing methods. Karthik *et al.* (2007) studied the degradation in mechanical properties of modified (mod) 9cr-1Mo steel on thermal aging at 923K using the small specimen test techniques viz., shear punch test and ball indentation test. Kang *et al.* (2006) proposed the finite element simulations to verify Tabor's empirical relations that enable the use of the indentation test for determination of post-yielding uniaxial stress-strain curves of a variety of ductile metallic alloys. Lee *et al.* (2008) introduced a method for deriving the tensile flow characteristics of austenitic materials from an instrumented indentation technique along with its experimental verification. Beghini *et al.* (2006) proposed a method for deducing the stress-strain uniaxial properties of metallic materials from instrumented spherical indentation. Hernot *et al.* (2006) established the relation between the penetration depth and the contact radius. It is required in order to determine the mechanical

properties of a material starting from an instrumented indentation test. Yan *et al.* (2006) presented dimensional analysis and the finite element method for the spherical indentation hardness of Shape Memory Alloys (SMAs). The scaling relationship between the hardness and the mechanical properties of SMAs, such as the forward transformation stress, the maximum transformation strain magnitude, has been derived. Elaguine *et al.* (2006) examined Hertzian fracture through experiments by the indentation of float glass specimens by steel balls. Yan *et al.* (2008) examined the indentation slope curve from a spherical indentation on elastic-plastic materials. Cao *et al.* (2007) developed a systematic method to determine the mechanical properties of materials using depth-sensing instrumented indentation tests, a key issue was to find the connection between the indentation response and the properties of the indented material. Bartier *et al.* (2010) studied the analytical models for the determination of the contact radius between a spherical indenter and an elastic-plastic material. Lee *et al.* (2010) studied spherical indentation based on numerical analysis and experiment, to develop thrust testing techniques to evaluate isotropic elastic-plastic material properties of metals. Sharm *et al.* (2011) presented a combined mechanical property evaluation methodology with automated ball indentation simulation and artificial neural network analysis is evolved to evaluate the mechanical properties for a carbon manganese steel and stainless steel.

Sathish Gandhi *et al.* (2012) presented the effect of tangent modulus in a contact parameters of a spherical ball contact with a flat plate. The different materials are considered for the study between E/Y=500 and 1750. Yaylac and Birinci (2013) studied the contact problem of two elastic layers with elastic constant and different height are considered for analysis. Kumaravelan *et al.* (2013) has discussed the design and contact analysis of leaf spring for two different cases such as single cantilever solid triangle beam and 3-beams of rectangular cross section for different materials. The detail reviewed of the spherical indentation process, it is identified that the study of spherical indentation through contact mechanics approach have not yet considered. Also the actual indentation depth and residual stress after unloading the indenter from end of the loading phase are not considered so far in the study. An attempt has been made for an analyzing the spherical indentation process through contact mechanics approach.

3. Materials and methods

In this model a rigid sphere is pressed against a deformable plate (flat) by applying a concentrated load on the center of the sphere. The analysis of spherical indentation of an elastic-plastic has been carried out using commercially available software 'ABAQUS'. The material properties are selected based on the Young's modulus and yield strength values. Table 1 shows the materials used for the applications of contact problems and hardness testing.

Table 1 Material properties

S. No.	Material	$E\times10^3$ N/mm^2	Y N/mm^2
1	Steel	210.83	200
2	Aluminium	70	130
3	Copper	125	125
4	Brass	105	135

3.1 Finite element modeling

Finite element contact model is created for indentation approach using 'ABAQUS' is based on the sphere and a flat contact method. In this model the assumptions were made for modeling such us the sphere is a rigid member, flat is a deformable member and frictionless contact between the indenter and flat. There are two methods for simulating the sphere and flat contact model. They are (i) load control and (ii) displacement control. In this analysis the displacement control is used for simulating the rigid sphere and a deformable flat. This method is suitable for analysing the model in 'ABAQUS' standard.

Fig. 2 shows the rigid sphere and a deformable flat contact model generated by using ABAQUS -6.9. The axisymmetric model is developed due to the advantage in the analysis procedure. The quarter sphere and half of the flat is considered the analysis based on the axisymmetric property of model. The sphere size of radius is 0.79375 mm (1/16 inch like in Brinell hardness test) and the flat size is 63 mm length and 10 mm thickness is considered for modeling (like Specimen size use for Brinell hardness test). In the modeling procedure the center of the rigid member (sphere) is taken as a Reference Point (RP).

3.2 Boundary condition and loading

Fig. 3 shows the boundary condition and loading for the simulation. The nodes lying on the axis of symmetry of the flat displacement are restricted to move in the radial direction (U1=UR3=0). Also the nodes in the bottom of the flat displacement are restricted to move in the

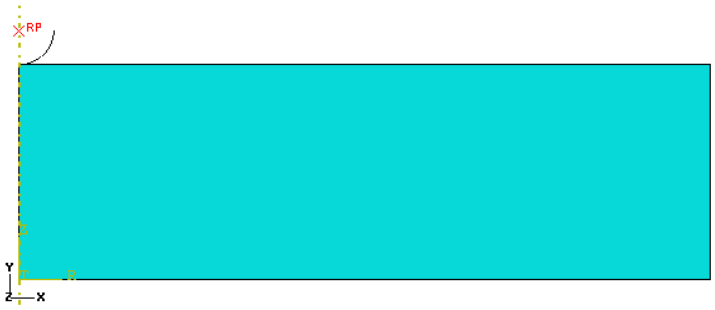

Fig. 2 Rigid sphere and a deformable flat contact model - ABAQUS

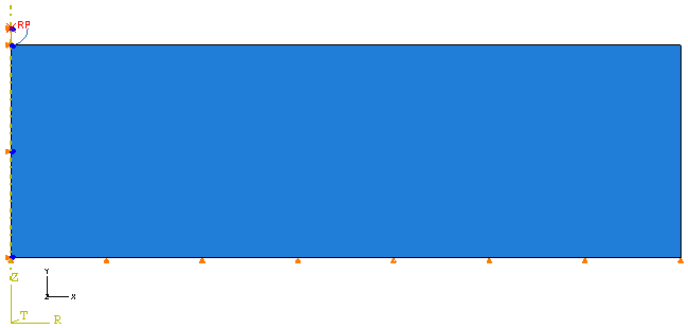

Fig. 3 Boundary conditions and loading

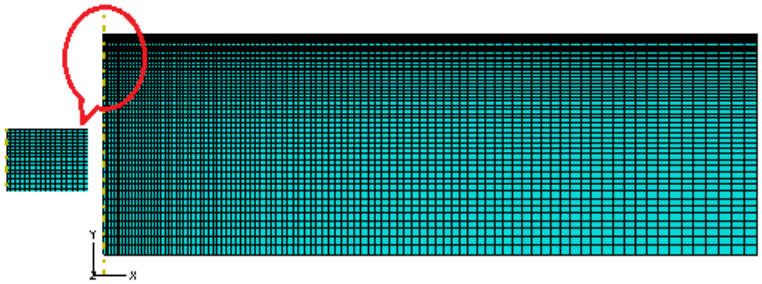

Fig. 4 Mesh generation - flat

vertical direction (U2=0). In the rigid surface the translations and rotations on a single node is known as rigid body reference node. In this model the reference point is assigned on the center of the indenter (sphere). The boundary conditions applied for this point are restricted to move in radial direction (U1=UR3=0).

The nodes lying on the axis of symmetry of the indenter and flat displacement is allowed in the vertical direction (U2≠0). For loading the displacement control method was applied. In this method the displacement is specified as input, which is equal to the penetrated depth of the sphere into a deformable flat.

3.3 Mesh generation

The edges of the flat (plate) are meshed by biased seed edges method. The finer mesh is generated around the indenter in order to encompass the region of the higher stress near the contact as shown in Fig. 4. The total number of elements and nodes generated in the flat is 5000 and 5151 respectively. The structured mesh was assigned, whereas biased mesh control. The element type of CAX4R type was used for all the simulations in which the letter or number indicates the type of element which is of Continuum type, Axisymmetric in nature has 4 nodes bilinear and Reduced integration with hour glass respectively.

3.4 Analysis of loading condition

The finite element simulation has been performed by using the condition of frictionless contact between the indenter and the flat for spherical indentation approach. The indentation process is assumed to be quasi-static approach, in which no time effect is considered. Hence ABAQUS - Standard method is used for indentation approach. The elastic-plastic material models is analyzed under loading condition of spherical indenter of radius 0.79375 mm. The objective of the analysis under this loading condition is to determine the indentation diameter for different materials and various contact parameters like contact pressure, Von-Mises stress, strain, equivalent plastic strain and reaction force in the indenter. The analysis has been performed for different materials like steel, aluminium, copper and brass. Here the simulation results of material steel is given.

3.4.1 Simulation output for steel

The following are the simulation output of steel material for an indentation depth of 0.18 mm in ABAQUS - Standard.

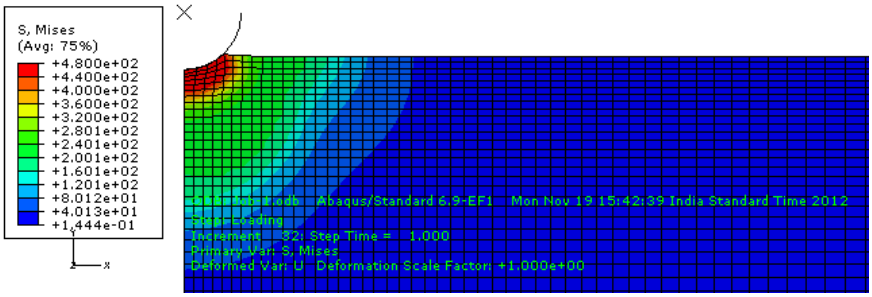

Fig. 5 Plot of Von-Mises stress in the deformed steel flat

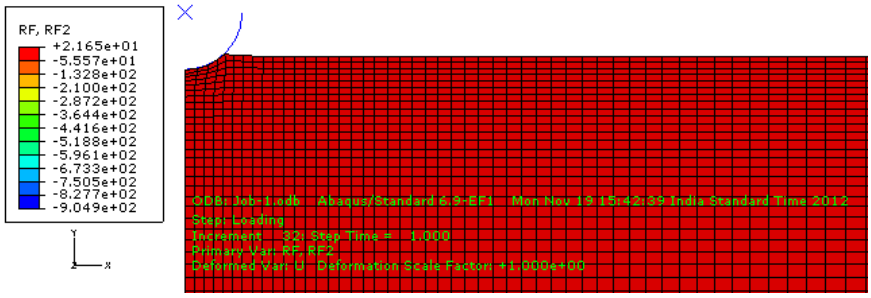

Fig. 6 Plot of reaction force in the spherical indentation into a steel flat

Fig. 5 shows the Von-Mises stress developed in the deformed flat. The maximum stress is developed in the contact region between indenter and the flat. The minimum stress is away from the contact region. The maximum and minimum stresses are 480 N/mm^2 and 0.1444 N/mm^2.

Fig. 6 shows the reaction force developed in the rigid spherical indenter. In the displacement control method, for the applied displacement the Reaction force (RF) on the indenter is the summation of force over the contact zone along the penetration direction. The reaction force in the indenter is 904.9 N.

3.5 Analysis of unloading condition (springback analysis)

The finite element simulation has been performed under unloading of the loaded spherical indenter into a flat. The penetrated indenter is return back to its initial position from the end of the indentation process is known as Springback analysis. In the springback simulation in which the material recovers its elastic deformation after the indenter is unloaded. This analysis is performed from the developed model in 'ABAQUS' for the loading condition by using the commands restart, copy model, edit attributes and so on. The main objective of this analysis is to determine the parameters which have not been studied in the experimental work like residual stress and strain.

3.5.1 Stress distribution simulation output for steel (Unloading)

The following are the simulation result of stress distribution for unloading the spherical indenter to bring back to its initial position. The model which is used in the loading condition of spherical indenter the same model is used and restart the results which is obtained in the loading step.

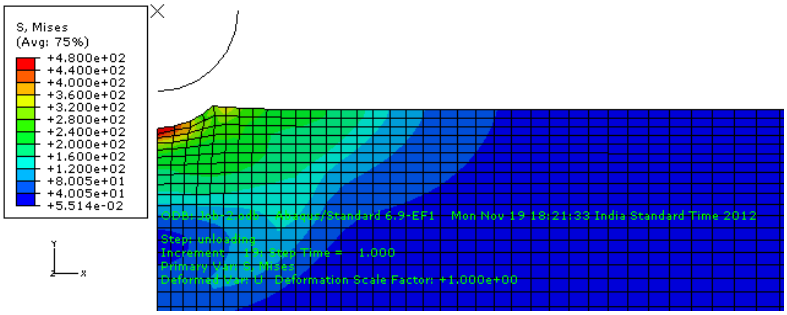

Fig. 7 Von-Mises stress plot of ateel flat after unloading

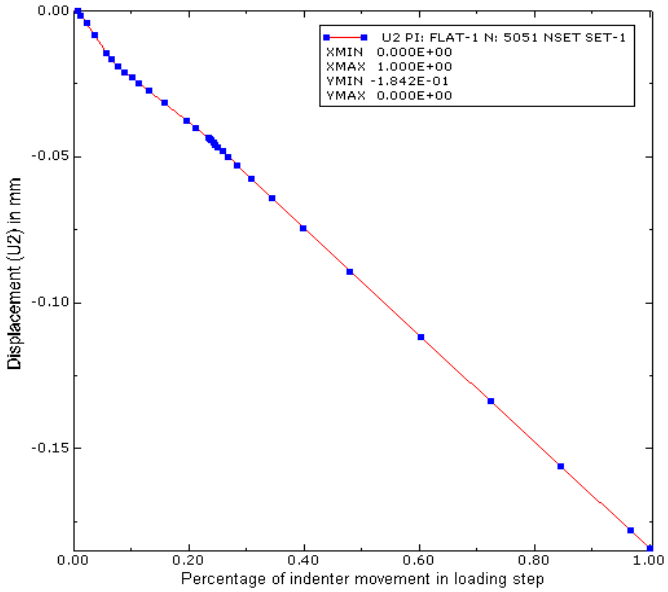

Fig. 8 Displacement of node 5051 in *Y*-direction in loading step-steel flat

Fig. 7 shows the Von-Mises stress distribution in the deformed steel flat after unloading. It is observed that the stress is released under the indenter and migrate into the left edge of the deformed flat after unloading. The value of maximum stress 480 N/mm^2 is same which is obtained in the loading step. But it is migrate to other location. The minimum stress outside the contact region is released from the flat after unloading.

It is important to analysis in this point, to study the behaviour of the displacement of the particular node in the left edge of the deformed flat. The further study has been carried out in such a node (Node number 5051). The study has focused on the displacement of the particular node in the loading and unloading steps. The displacement of the indenter is same as that of in the loading case of steel material.

Fig. 8 shows the simulation output plot of displacement of node 5051 in the loading step. This plot gives the relationship between the displacement of node in the direction of indenter penetration and percentage of indenter movement into a steel flat. It shows that for the complete movement of indenter the node displaced at a distance of 0.1842 mm.

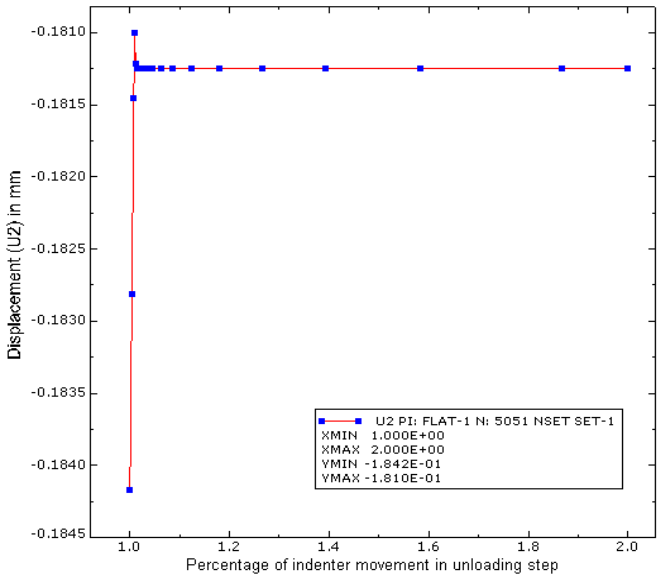

Fig. 9 Displacement of node 5051 in Y-direction in unloading step-steel flat

Fig. 9 shows the simulation output plot of displacement of node 5051 in the unloading step. This plot gives the relationship between the displacement of node in the direction opposite to the indenter penetration and percentage of indenter movement in unloading step of steel flat. It shows that for 100% of unloading the particular node is displaced from 0.1842 mm to 0.18125 mm and for further unloading the node displacement is constant.

4. Experimental work

Experiments are carried out for indentation approaches contact models to study the behaviour of the contact bodies in the nature of contact and load applied to the model. The work has been carried out for indentation diameter and depth of indentation for an spherical indentation process.

4.1 Indentation diameter measurement

The spherical indentation experimental study has been carried out for indentation model in Brinell Hardness tester for different materials like steel, aluminium, copper and brass. The main objective of this study is to determine how the indentation diameter is varying for the different material of an identical load, size of the indenter and time. The spherical indentation testing is carried out in a spherical indenter of size 1.5875 mm diameter, an applied load of 1000 N and the specimen size of 63 mm×10 mm flat plate. The load is applied for a maximum period of 30 second.

The Fig. 10 shows that, the residual indentation of a spherical indentation testing in the steel flat. The diameter of the residual indentation is measured as 0.95 mm. Fig. 10 shows that, when the spherical indenter penetrated into a Aluminium flat, it observed that the bulged material between the indenter and the flat is pile-up around the circumference of the indentation area. The

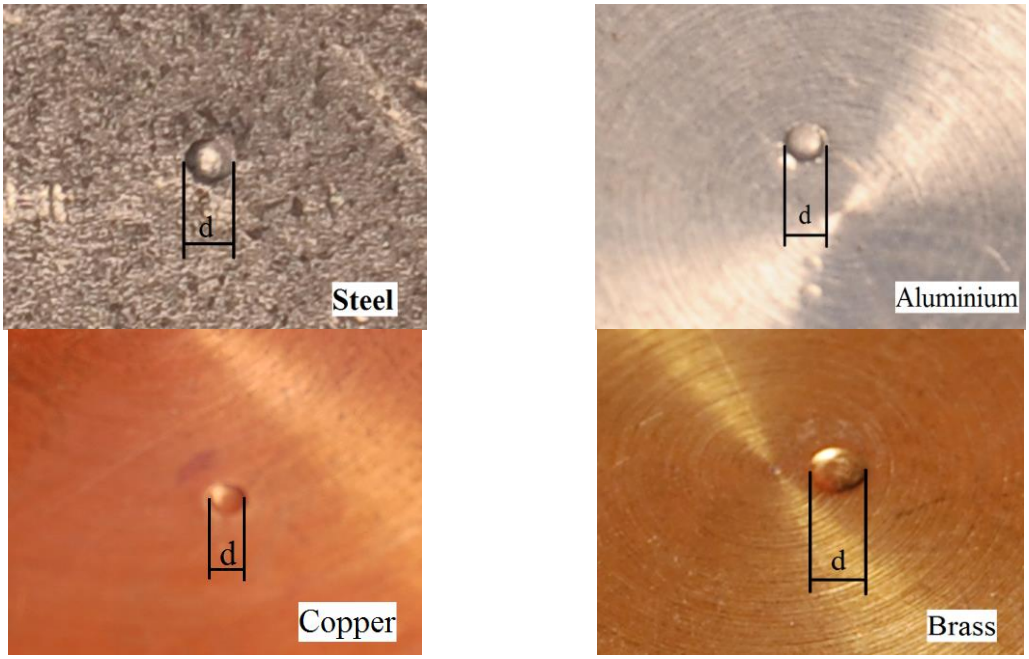

Fig. 10 Residual indentation diameters - Steel, Aluminium, Copper and Brass

Fig. 11 Dial indicator setup

diameter of the residual indentation is measured as 1.45 mm.

Fig. 10 shows that, when the spherical indenter penetrated into a copper flat, it observed that the bulged material between the indenter and the flat is pile-up around the circumference of the indentation area is less than the aluminium. The diameter of the residual indentation is measured as 1.20 mm. Fig. 10 shows that, when the spherical indenter penetrated into a brass flat, it observed that the bulged material between the indenter and the flat is pile-up around the

Table 2 Depth of indentation for different materials

S. No.	Material	Depth of indentation experiment (mm)
1	Steel	0.20
2	Aluminium	0.55
3.	Copper	0.45
4.	Brass	0.32

circumference of the indentation area is less than the copper. The diameter of the residual indentation is measured as 1.15 mm.

4.2 Indentation depth measurement

Fig. 11 shows a dial indicator apparatus setup for a spherical indentation depth measurement.

The hard indenter penetrated into a deformable specimen the depth of penetration is occurred in a specimen. Initially the dial indicator plunger is placed in an indentation part and set a reference point as zero in a dial gauge. Then the gauge is move into a surface of the specimen near to the indentation portion. The gauge shows the depth of penetration of the indentation part. Likewise the depth of penetration for different materials like steel, aluminium, copper and brass are measured and shown in the Table 2. It shows the depth of indentation for an experimental and simulation results. These values are within the acceptable range.

5. Results and discussion

The contact analysis of an elastic-plastic model of a sphere and a flat contact has been carried out by an indentation approaches. Finite element software "ABAQUS" is employed to simulate the model and the results are an experimentally verified.

5.1 Analysis of spherical indentation process during loading

The simulation was performed in the 'ABAQUS' software for a spherical indentation process for different materials like Steel, Aluminium, Copper and Brass at different indentation depth. The indentation diameter and reaction force were measured for all the materials. The experiments were conducted in the Brinell hardness testing machine for an indentation process and the indentation diameters were measured. The experimental results are compared with the simulation results is shown in Table 3 and observed that the deviation is within ±3.16%. Hence it is in the acceptable range.

Fig. 12 shows the relation between the indentation diameter (simulation and experiment) and depth of indentation for different materials. The indentation diameter obtained from experimental study is almost same as the diameter obtained from the finite element simulation results. It shows that, the indentation diameter is depends on the depth of indentation. It is also very important to analyse the indentation diameter with respect to the reaction force developed in the indenter.

Fig. 13 shows the relation between the average indentation diameter and reaction force (simulation and experiment) for different materials. It is observed that, the indentation diameter is

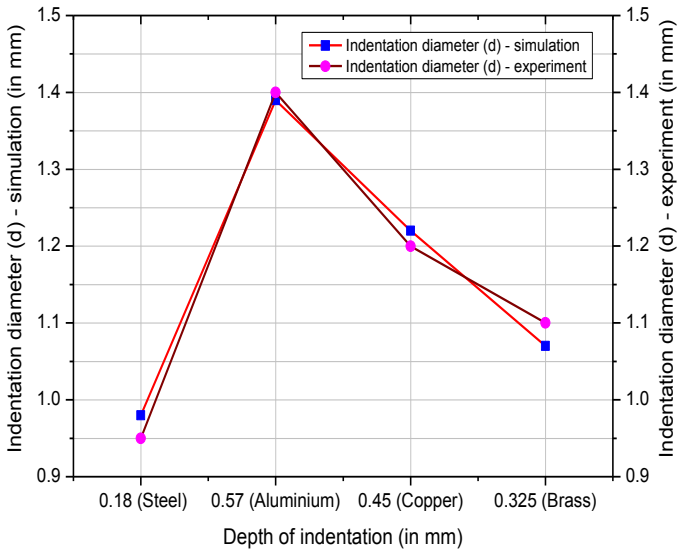

Fig. 12 Indentation diameter-simulation and experiment Vs. depth of indentation for different materials

Table 3 Residual indentation diameter - FEA and Experiment

S. No.	Material	Residual indentation diameter (d) in FEA (mm)	Residual indentation diameter (d) in experiment (mm)	Percentage deviation
1	Steel	0.98	0.95	-3.16
2	Aluminium	1.39	1.40	0.71
3.	Copper	1.22	1.20	-1.67
4.	Brass	1.07	1.10	2.73

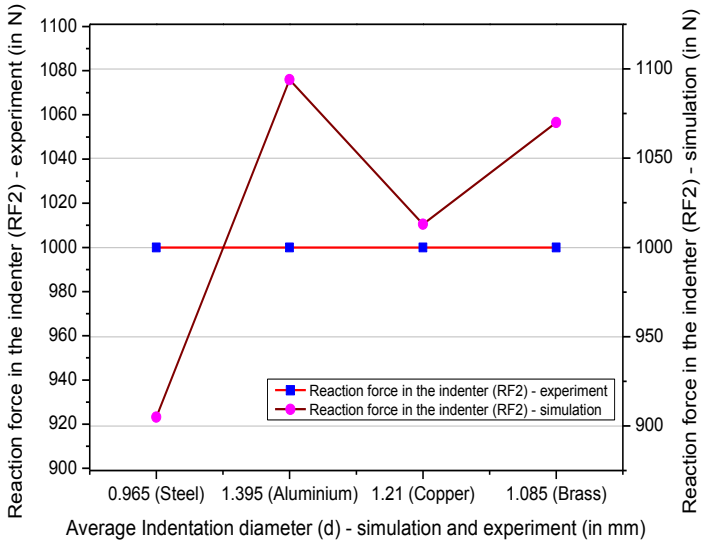

Fig. 13 Reaction force (RF2) Vs average indentation diameter - simulation and experiment

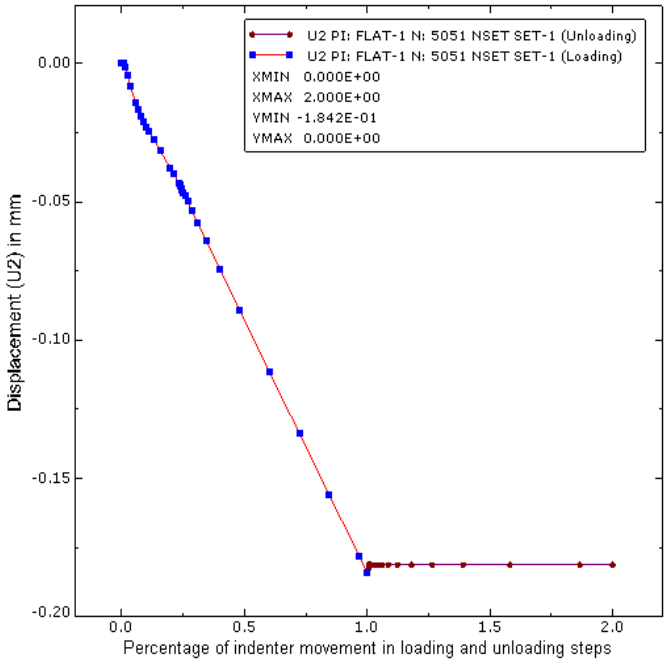

Fig. 14 Displacement of node 5051 in Y-direction in loading and unloading steps-steel flat

not completely depends on load applied for the indentation process, it also depends on the material properties of the indentation specimen. The study of indentation depth with respect to the load applied for different materials is further considered for discussion.

5.2 Analysis of spherical indentation process during unloading

Fig. 14 shows the simulation output plot of displacement of node 5051 in loading and unloading step. It shows that at the end of the loading step the node reached the maximum displacement of 0.1842 mm. It has been slightly greater than the applied displacement in the indenter (0.18 mm). At the starting of the unloading step the node displaced at a distance of 0.00295 mm in the upward direction and then no further displacement in the node. It is clear that the indentation depth is increased by 0.00125 mm than the applied once.

5.2.1 Comparison of actual indentation depth for different materials

The loading and unloading process has been carried out for all the materials like steel, aluminium, copper and brass. The increase in the indentation depth for these materials as shown in Table 4.

From the Table 4 it is stated that the actual indentation depth after unloading is high in the low yield strength material and low in the high yield strength material.

Fig. 15 clearly shown that, the actual indentation depth after unloading the spherical indenter is greater in the low yield strength material like aluminium and copper. The result shows that the actual indentation depth in the indentation process is slightly greater than the displacement of the indenter applied into a flat.

Table 4 Increase in the indentation depth for all materials

S. No.	Materials	Indenter displacement applied, (U2) (mm)	Node (5051) displacement, (U2)		Actual indentation depth after unloading (mm)
			Loading step (mm)	Increased by after unloading step, (mm)	
1	Steel	0.18	0.1842	0.00125	0.18125
2	Aluminium	0.57	0.5926	0.0121	0.5821
3	Copper	0.45	0.4616	0.0056	0.4556
4	Brass	0.325	0.3314	0.0022	0.3272

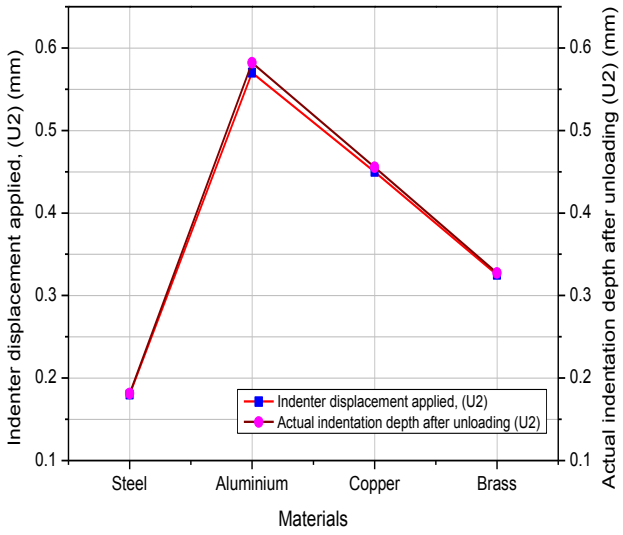

Fig. 15 Indenter displacement applied and actual indentation after unloading Vs materials

Table 5 Comparison of different parameters for different materials

S. No.	Material	Von-Mises Stress	Strain	Contact pressure	Reaction force	Equivalent plastic strain	Depth of penetration	Indentation diameter
		N/mm^2	-	N/mm^2	N	-	mm	mm
1	Aluminium	237.5	1.879	720	1094	2.084	0.57	1.39
2	Copper	275	0.253	863.6	1013	1.554	0.45	1.22
3	Brass	350	0.955	1191	1070	1.029	0.325	1.07
4	Steel	480	0.567	1196	904.9	0.6373	0.18	0.98

5.3 Comparison of different parameters for different materials

The comparison has been made for different parameters like stress, strain, contact pressure, reaction force, equivalent plastic strain, depth of penetration and pile-up height for different materials like steel, aluminium, copper and brass.

Table 5 shows the comparison of different parameters like Von-Mises stress, strain, contact pressure, reaction force, equivalent plastic strain, depth of penetration and indentation diameter are measured from the simulation for different materials. It shows that, the indentation diameter

decreases with the increases in the stress and contact pressure, due to the decreases in area of contact. The parameters like strain, equivalent plastic strain and depth of penetration getting decreased due to the decrease in area of contact. It is observed that the parameters which are increasing are inversely proportional to the area of contact and all other parameters expect reaction force are directly proportional to the area of contact. The reaction force depend on the hardness of the indenter material and it is related to the load applied for indentation process.

6. Conclusions

The simulation has been performed in the 'ABAQUS' software for a spherical indentation model. The analysis was carried out for the different materials like steel, aluminium, copper and brass at different indentation depth under loading and unloading conditions. The reaction force of the rigid indenter and indentation diameter are estimated in the loading condition and compared with experimental work. It is observed that, the indentation diameter is not completely depends on the load applied for the indentation process it also depends on the material properties of the indentation specimen. The analysis has been extended to the depth of indentation during loading and unloading conditions for different materials like steel, aluminium, copper and brass. So that the springback (unloading) analysis has been performed to recovers the elastic property of the material and the stress and distribution are investigated in the indentation area. The springback analysis results shows that the actual indentation depth is slightly greater than the depth of penetration of the indenter applied.

References

Ahn, J.H. and Kwon, D. (2001), "Derivation of plastic stress-strain relationship from ball indentation: Examination of strain definition and pileup effect", *J. Mater. Res.*, **16**(11), 3170-3178.

Bartier, O., Hernot, X. and Mauvoisin, G. (2010), "Theoretical and experimental analysis of contact radius for spherical indentation", *Mech. Mater.*, **42**, 640-656.

Beghini, M., Bertini, L. and Fontanari, V. (2006), "Evaluation of the stress-strain curve of metallic materials by spherical indentation", *Int. J. Sol. Struct.*, **43**, 2441-2459.

Bisrat, Y. and Roberts, S.G. (2000), "Residual stress measurement by Hertzian indentation", *Mater. Sci. Eng. A*, **288**, 148-153.

Cao, Y.P. and Lu, J. (2004), "A new method to extract the plastic properties of metal materials from an instrumented spherical indentation loading curve", *Acta Materialia*, **52**, 4023-4032.

Cao, Y., Qian, X. and Huber, N. (2007), "Spherical indentation into elastoplastic materials: Indentation-response based definitions of the representative strain", *Mater. Sci. Eng. A*, **454**(455), 1-13.

Demir, A. and Sonmez, F.O. (2004), "Predication of Brinell hardness distribution in cold formed parts", *ASME J. Eng. Mater. Tech.*, **126**, 398-405.

Elaguine, D., Brudieu, M.A. and Storakers, B. (2006), "Hertzain fracture at unloading", *J. Mech. Phys. Solid.*, **54**, 2453 - 2473.

Habbab, H., Mellor, B.G. and Syngellakis, S. (2006), "Post-Yield characterisation of metals with significant pile-up through spherical indentations", *Acta Materialia*, **54**, 1965 - 1973.

Hernot, X., Bartier, O., Bekouche, Y., El Abdi, R. and Mauvoisin, G. (2006), "Influence of penetration depth and mechanical properties on contact radius determination for spherical indentation", *Int. J. Sol. Struct.*, **43**, 4136-4153.

Kang, B.S.J., Yao, Z. and Barbero, E.J. (2006), "Post-yielding stress-strain determination using spherical

indentation", *Mech. Adv. Mater. Struct.*, **13**(2), 129-138.
Karthik, V., Laha, K., Parameswaran, P., Kasiviswanathan, K.V. and Baldevraj, (2007), "Small specimen test techniques for estimating the tensile property degradation of Mod 9cr-iMo steel on thermal aging", *J. Test. Eval.*, **35**(4), 438-448.
Kumaravelan, R., Ramesh, S., Sathish Gandhi, V.C., Joemax Agu, M. and Thanmanaselvi, M. (2013), "Analysis of multi leaf spring based on contact mechanics- a novel approach", *Struct. Eng. Mech.*, **47**(3), 443-454.
Lee, H., Lee, J.H. and Pharr, G.M. (2005), "A numerical approach to spherical indentation techniques for material property evaluation", *J. Mech. Phys. Solid.*, **53**, 2037-2069.
Lee, K.W., Kim, K.H., Kim, J.Y. and Kwon, D. (2008), "Derivation of tensile flow characteristics for austenitic materials from instrumented indentation technique", *J. Phys. D, Appl. Phys.*, **41**, 074041.
Lee, J.H., Kim, T. and Lee, H. (2010), "A study on robust indentation techniques to evaluate elastic-plastic properties of metals", *Int. J. Solid. Struct.*, **47**, 647-664.
Sathish Gandhi, V.C., Ramesh, S., Kumaravelan, R. and Thanmanaselvi, M. (2012), "Contact analysis of spherical ball and a deformable flat model with the effect of tangent modulus", *Struct. Eng. Mech.*, **44**(1), 61-72.
Sharm, K., Bhasin, V., Vaze, K.K. and Ghosh, A.K. (2011), "Numerical simulation with finite element and artificial neural network of ball indentation for mechanical property estimation", *Sadhana Ind. Acad. Sci.*, **36**(2), 181-192.
Yan, W., Sun, Q. and Liu, H.Y. (2006), "Spherical indentation hardness of shape memory alloys", *Mater. Sci. Eng. A*, **425**, 278 - 285.
Yan, W., Sun, Q. and Hodgson, P.D. (2008), "Determination of plastic yield stress from spherical indentation slop curve", *Mater. Let.*, **62**, 2260-2262.
Yaylac, M. and Birinci, A. (2013), "The receding contact problem of two elastic layers supported by two elastic quarter planes", *Struct. Eng. Mech.*, **48**(2), 241-255.

CC